

EDO-Net: Learning Elastic Properties of Deformable Objects from Graph Dynamics

Alberta Longhini^{*1}, Marco Moletta^{*1}, Alfredo Reichlin¹, Michael C. Welle¹,
David Held², Zackory Erickson², and Danica Kragic¹

Abstract— We study the problem of learning graph dynamics of deformable objects which generalize to unknown physical properties. In particular, we leverage a latent representation of elastic physical properties of cloth-like deformable objects which we explore through a pulling interaction. We propose EDO-Net (*Elastic Deformable Object - Net*), a model trained in a self-supervised fashion on a large variety of samples with different elastic properties. EDO-Net jointly learns an *adaptation* module, responsible for extracting a latent representation of the physical properties of the object, and a *forward-dynamics* module, which leverages the latent representation to predict future states of cloth-like objects, represented as graphs. We evaluate EDO-Net both in simulation and real world, assessing its capabilities of: 1) generalizing to *unknown* physical properties of cloth-like deformable objects, 2) transferring the learned representation to new downstream tasks.

I. INTRODUCTION

Manipulation of deformable objects is a fundamental skill toward folding clothes, assistive dressing, wrapping or packaging [1], [2], [3], [4]. In unstructured environments, variations in physical properties such as mass, friction, density or elasticity influences the dynamics of the manipulation [5], [6]. Modelling, learning and transferring skills considering deformable objects remain open challenges in robotics [7] and are due to two key factors: *i*) the state of deformable objects is high dimensional and difficult to represent canonically; *ii*) the interaction dynamics are often non-linear and influenced by the objects' physical properties usually not known a-priori [8].

To address *i*), analytical models often employ particle-based representations such as graphs, commonly extracted from point clouds [9], [10], [11]. Recent advances in Graph Neural Network (GNN) research have shown promising results in learning complex physical systems [12], [13], [14]. However, current methods assume that the physical properties are known a-priori, which may not hold when it comes to robots operating in human environments, requiring to address problem *ii*). The field of *intuitive physics* [15] tackles this challenge by learning predictive models which distill knowledge about the physical properties from past experience and interaction observations [16]. This line of research has so far focused mostly on rigid objects, but recent advances of data-driven techniques for deformable objects

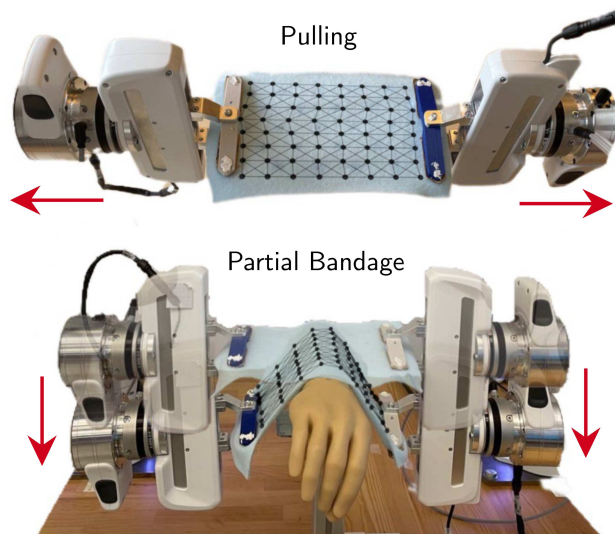


Fig. 1: A pulling interaction is leveraged by EDO-Net to explore the elastic properties of the object, which improves performance in subsequent task such as partial bandage.

manipulation suggest that interactions such as whipping or pulling may be relevant to learn an intuitive physics model of deformable objects [8], [17].

In this paper, we study the problem of learning graph dynamics of deformable objects that generalize to objects with unknown physical properties. In particular, we focus on elastic properties of cloth-like deformable objects, such as textiles, which we explore through a pulling interaction (Fig. 1). We propose EDO-Net (*Elastic Deformable Object - Net*), a model trained in a self-supervised fashion on a large variety of samples with different elastic properties. EDO-Net jointly learns an *adaptation* module, responsible for extracting a latent representation of the physical properties of the object, and a *forward-dynamics* module, which leverages the latent representation to predict future states, represented as graphs.

We evaluate our approach both in simulation and in the real world, showing how EDO-Net accurately predicts the future states of a deformable object. We also validate the quality of the learned representation by retrieving the ground truth physical properties from the simulation environment using a weak learner. In summary, our contributions are:

- We propose EDO-Net, a model to learn a latent representation of physical properties of cloth-like deformable objects without explicit supervision, as well as their

^{*}Contributed equally (listed in alphabetical order)

¹The authors are with the Robotics, Perception and Learning Lab, EECS, at KTH Royal Institute of Technology, Stockholm, Sweden [albertal](mailto:albertal@kth.se), [moletta](mailto:moletta@kth.se), [alfrei](mailto:alfrei@kth.se), [mwelle](mailto:mwelle@kth.se), dani@kth.se

²The authors are with are with Carnegie Mellon University, Pittsburgh, USA [dheld](mailto:dheld@cmu.edu), zerickso@andrew.cmu.edu

graph dynamics;

- We propose a procedure to train our model on a large variety of samples with different elastic properties, enabling generalization to objects with *unknown* physical properties;
- We conduct extensive evaluations, both in simulation and in the real world, of the quality of the latent representation and of the dynamics prediction.

II. RELATED WORK

We discuss the related work from the perspective of learning physical properties, as well as data-driven strategies to learn representations and dynamics of deformable objects.

Learning physical properties: a common approach to extract physical properties like mass, moment of inertia or friction coefficients is to use different exploratory actions such as pushing, tilting or shaking [6], [18], [5]. In [6] mass and friction of rigid objects are learned through tactile exploration. Similarly, [19], [5] use a multi-step framework to encode rigid objects physical properties from pushing tasks using dense pixels representations. Related to deformable objects, in [20] the authors propose how to predict properties of cloth-like objects to perform real2sim, learning to align real world and simulated behaviors through a differentiable simulator. In contrast to [20], we want to learn a representation of physical properties without relying on simulated behaviors and elastic parameters.

Representations and dynamics of deformable objects: regarding the challenge of finding canonical representations of deformable objects, an approach is to encode their high dimensional observations in structured latent spaces to perform planning and control there. An example is [21], where the authors use contrastive learning on image observations to separate different states in the latent space to learn how to manipulate deformable objects such as clothes and ropes. Similarly, in [22], [23], image observations are mapped in a latent space represented as a graph, where similar observations are mapped to the same nodes, allowing to perform visual action planning to solve a folding task with clothes. G-Doom [11], instead, relies on a graph representation to learn cloth-like deformable objects dynamics directly using GNNs. VCD [10] is a cloth dynamics model based on particle representations and connectivity structure of the visible portion of the cloth which addresses the challenge of partial observations. DiffSRL [24] proposes to introduce a physics prior relying on a differentiable simulator to better capture the complex dynamics models of deformable objects. None of these works, however, focus on learning graph dynamics across a wide range of physical properties of deformable objects. To the best of our knowledge, this is the first work to propose a method that explicitly trains a graph dynamics model to generalize to unknown physical properties of cloth-like deformable objects.

III. PROBLEM FORMULATION

In our formulation, we refer to the object’s elastic properties as $\mathcal{T}_i \sim \mathcal{T}$, where \mathcal{T} is the distribution of all possible

physical properties. We explore \mathcal{T}_i by collecting a sequence of observations O^i through an Exploratory Action (EA) [5], [6]. An *adaptation module* is responsible for extracting a latent representation z_i of the physical properties \mathcal{T}_i from the observations O^i , which can be subsequently leveraged by a *forward dynamics module* to generalize its predictions across different $\mathcal{T}_i \sim \mathcal{T}$. We define the state of a deformable object with physical properties \mathcal{T}_i as a graph $G^i = (V^i, E^i)$ with nodes $v \in V^i$ and edges $e \in E^i$. The features of the node v describe the 3D Cartesian position of the nodes, while the features of the edge e characterize the interaction properties among nodes.

Given these, the aim of EDO-Net is to learn a graph dynamics model of cloth-like deformable objects g_θ conditioned on a latent representation z_i of the underlying physical properties \mathcal{T}_i of the deformable object and the robot control action a_t :

$$\delta \hat{G}_t^i = g_\theta(G_t^i, a_t, z_i). \quad (1)$$

The latent representation z_i can be obtained through a learned function f_ϕ that takes as input sequence of observations O^i and an initialization z_0 of the representation:

$$z_i = f_\phi(O^i, z_0), \quad (2)$$

where the initialization z_0 is learned together with the model’s parameters θ and ϕ . In what follows, we will describe in detail the method to implement and train the graph dynamics g_θ and adaptation functions f_ϕ , respectively.

IV. METHOD

An overview of the proposed EDO-Net is shown in Fig. 2. In particular, for each deformable object with unknown physical properties \mathcal{T}_i , the robot has to adapt the initialization z_0 by using a sequence of exploratory observations O^i . From O^i , the adaptation module f_ϕ first extracts a latent representation z_i of the physical properties \mathcal{T}_i . The extracted representation z_i is subsequently used in the forward dynamics module g_θ to obtain accurate predictions of the future states of \mathcal{T}_i conditioned on different interactions a_t .

We assume that the state G_t^i of the deformable object with physical properties \mathcal{T}_i is directly observable, which, in real-world applications, can be extracted from observations such as point clouds [11], [10]. We focus on the scenario where the physical properties \mathcal{T}_i are not directly observable from the initial state of the object.

A. Exploratory Action and Adaptation

To collect information about the physical properties \mathcal{T}_i , the robot needs to observe the response of the object during a dynamic interaction. To this end, we evaluate a *pulling* interaction shown in Fig. 3, where a two-arm robotic manipulator grasping a deformable object from its edges exerts tension stress on the object by pulling its edges along opposite directions, similarly to what is done in [17]. During the pulling Exploratory Action (EA), we record a set of T observations $O^i = O_t^i |_{t=1, \dots, T}$ where each $O_t^i = (G_t^{O^i}, F_t^{O^i})$ consist of the object state $G_t^{O^i}$ and the force $F_t^{O^i}$ recorded from

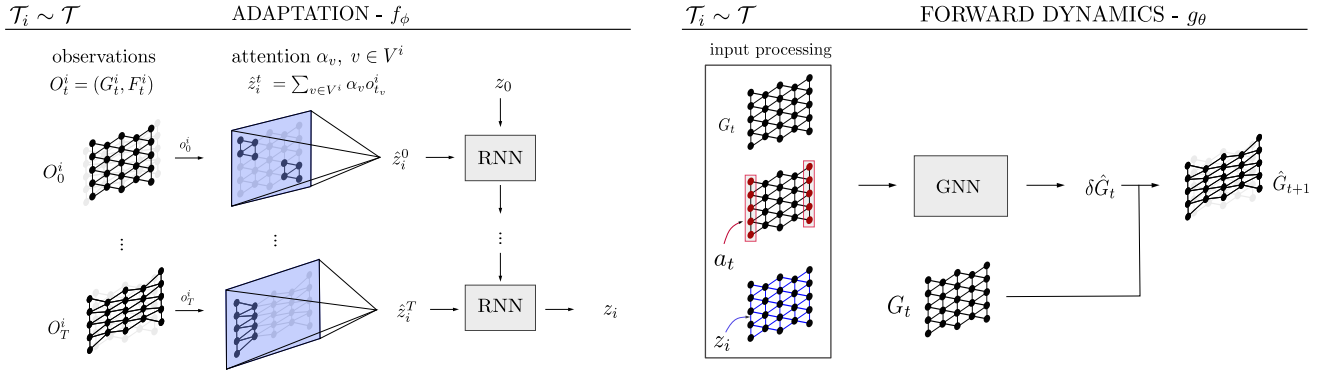


Fig. 2: Scheme of the overall model. Given a deformable object \mathcal{T}_i with *unknown* physical properties, the adaptation module f_ϕ updates the initialization z_0 of the latent representation of the physical properties \mathcal{T}_i from sequences of observations $O_t^i|_{t=1,\dots,T}$ processed by an attention layer and a RNN. In a second phase, the forward dynamics module g_θ , implemented as a GNN, uses z_i obtained from the adaptation module to predict future states \hat{G}_t of the deformable object.

the robot sensors at time t . The information contained in O^i about the physical properties \mathcal{T}_i is subsequently input to the learned function f_ϕ to update the initialization z_0 . The implementation of the adaptation function f_ϕ is the following: for each observation O_t^i , we encode $(G_t^{O^i}, F_t^{O^i})$ into a latent embedding o_t^i through a Multi-Layer Perceptron (MLP). We subsequently obtain an estimate $\hat{z}_t^i \in \mathbb{R}^p$ of z_i from o_t^i by learning a node’s aggregation function through an attention layer, which aggregates the nodes as [25]:

$$\hat{z}_t^i = \sum_{v \in V^i} \alpha_n o_{t,v}^i, \quad (3)$$

where α_n is the attention weight of the node n . For details about the implementation of the attention mechanism, we refer the reader to [26]. The set of $\hat{z}_t^i |_{t=1,\dots,T}$ is used to obtain the latent representation $z_i \in \mathbb{R}^p$ by recursively updating the initial belief z_0 through a Recurrent Neural Network (RNN), yielding the following update rule:

$$z_i = \text{RNN}(\hat{z}_t^i |_{t=1,\dots,T}, z_0). \quad (4)$$

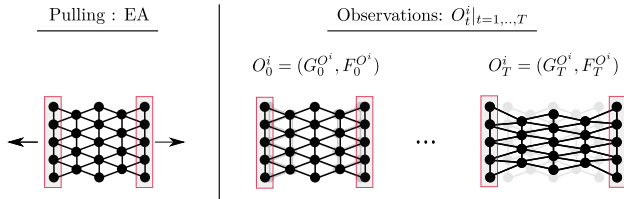


Fig. 3: Exploration Actions - Pulling to observe graphs and forces

B. Forward Dynamics Module

We model the forward graph dynamics g_θ with a GNN conditioned on the latent representation z_i of the physical properties \mathcal{T}_i . We trained g_θ to predict state differences δG_t^i receiving as input the control action of the robotic manipulator a_t , and the initial state of the object G_t^i . We integrate z_i as features of the edges of the input graph as shown in the *input processing* block in Fig. 2. We use MLPs to encode nodes and edges before propagating the information among

the nodes using a standard M -step message passing GNN with the following update rule [27]:

$$h_v^m = \Phi \left(\sum_{s \in \mathcal{N}_v^1 \cup \mathcal{N}_v^2} \Psi(h_v^{m-1}, h_s^{m-1}, z_i) \right) \quad \forall v \in V^i, \quad (5)$$

where Ψ and Φ are the learned message and update functions, and \mathcal{N}_v^1 and \mathcal{N}_v^2 are the sets of 1st and 2nd order neighbors of the node $v \in V^i$. To decrease the number of steps needed to propagate the information along the graph, we parallelize the computation of 1st and 2nd order neighbors as suggested in prior work [28]. Finally, the M -th hidden nodes are passed through a decoder MLP to the prediction of the graph displacement $\delta \hat{G}_t^i$.

C. Self-Supervised Loss

The overall model can be learned using a dataset of exploratory observations $\mathcal{D}^O = \{D^{O^i}\}_{\mathcal{T}_i \sim \mathcal{T}}$ and a dataset of interactions $\mathcal{D} = \{D_i\}_{\mathcal{T}_i \sim \mathcal{T}}$. The parameters ϕ , θ and the initialization z_0 can be optimized using a loss on the prediction of the state difference $\delta \hat{G}_t^i$ obtained from g_θ for each training sample with physical properties $\mathcal{T}_i \sim \mathcal{T}$. The loss function \mathcal{L} can be defined as follows:

$$\mathcal{L} = \mathbb{E}_{\substack{\mathcal{T}_i \sim \mathcal{T} \\ G_t^i, a_t, \delta G_t^i \sim \mathcal{D}_i}} [d(\delta \hat{G}_t^i, g_\theta(G_t^i, a_t, z_i))], \quad (6)$$

where $z_i = f_\phi(O^i, z_0)$ with $O^i \sim \mathcal{D}^O$, and d is a distance measure, Mean-Squared Error (MSE), between the ground truth state displacement of the deformable object and the model’s prediction. Equation 6 optimizes the parameters θ to learn a forward dynamic model conditioned on different representations z_i of physical properties \mathcal{T}_i , implicitly driving the parameters ϕ to learn to encode z_i of different samples without supervision from ground truth labels of the physical parameters. Moreover, training across multiple $\mathcal{T}_i \sim \mathcal{T}$ enforces the model to learn how to generalize to deformable objects with unknown physical properties.

V. ENVIRONMENT AND IMPLEMENTATION DETAILS

In this section, we introduce the simulated and real-world environments designed to evaluate the proposed method, along with its implementation and training details.

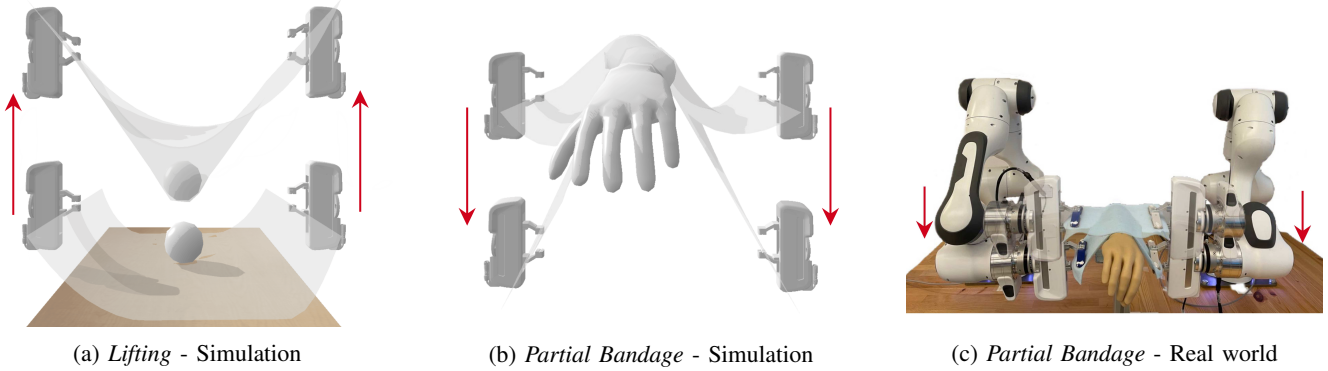


Fig. 4: The environments employed to evaluate EDO-Net.

A. Environments Setup

For the simulation experiments, we use Pybullet [29], [30]. In it, we create the two environments displayed in Fig. 4a and Fig. 4b, both of which include two free-floating Franka-Emika Panda end-effectors equipped with Force/Torque sensors. In the first environment, called *Lifting*, the robot lifts a sphere located on a cloth-like deformable object from an initial resting position on the table to a predefined height, by applying a displacement control action $a_t \in [0, D_{max}]$. In the second environment, called *Partial Bandage*, the robot holds and pulls the cloth downward over a human arm, applying a force control action $a_t \in [0, F_{max}]$. For both environments, we uniformly discretize the action intervals into 30 instances with fixed step size, while the pulling EA is implemented as shown in Fig. 3.

We extract the graph G_t^i and force F_t^i observations at each time step of the simulation. We downsample the graph to a grid of 8×8 nodes. Furthermore, we smooth the force profiles using a Savitzky–Golay filter [31] with a window size of 21 and a third-grade polynomial.

We generate a large variety of physical properties of the cloth by varying both the *stiffness* and the *bending* parameters of the simulator. We empirically selected the elasticity parameters in the range $[10, 45]$ with a step size of 3.0, and the bending parameters in the range $[0.01, 5.01]$ with a step size of 0.5, for a total of 143 unique elastic deformable objects.

We replicate the *Partial Bandage* simulation environment in the real world as visible in Fig. 4c. We collect the pulling EA and the interaction trajectories on 40 different textile samples with different elastic properties where the dataset characteristics correspond to the one in prior work [32]. The real-world dataset and the graph extraction procedure are shown in Fig. 5.

B. Network Architecture and Training details

We used an MLP with one hidden layer of size 32 to implement the node encoder of the adaptation module, while the attention layer is implemented as a learned linear projection from the encoded node $o_v \in \mathbb{R}^{32}$ to the attention value $\alpha_v \in \mathbb{R}$. The RNN architecture has one hidden state which starts with initialization $z_0 \in \mathbb{R}^p$ and outputs $z_i \in \mathbb{R}^p$ as its last hidden state [33], where $p = 32$. Hyperparameters were

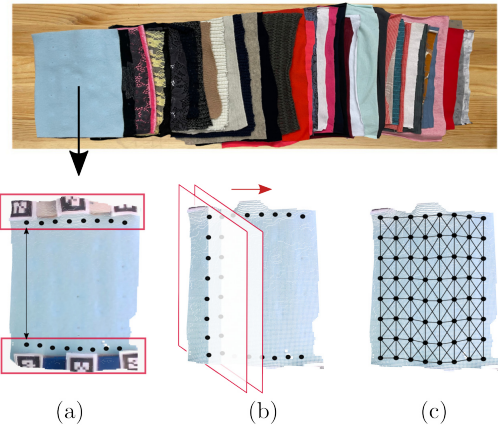


Fig. 5: Textile dataset samples (top) and procedure to extract graphs from point cloud (bottom). First we localize the gripper and represent them as a set of 8 equidistant nodes (a). We then slice the point cloud with a plane for 2 corresponding nodes on the grippers, obtaining 6 additional equidistant nodes (b). We obtain the final graph by defining the neighbors of each node segment (c).

chosen empirically based on the highest overall performance across the evaluations. Regarding the forward model, we propagate the information for $M = 4$ steps, while we implement the node’s encoder, the final linear projection, and the message and the aggregation functions as MLPs with one hidden layer of size 32. We use ReLU as non-linearity for all the modules except the RNN, where we used tanh as the activation function. The models are trained on the datasets normalized to zero mean and unit variance for $5K$ epochs and batch size equal to 8. We used Adam [34] with a learning rate of 10^{-3} and weight decay equal to 10^{-5} . The simulation dataset consists of 30 datapoints for each of the 143 unique samples for *Lifting*, *Partial Bandage* and the pulling EA. We split the 143 samples into a train (80%), validation (10%), and test (10%) samples, using the validation set to select the best-performing model during training. In the real world, instead, the dataset consists of 30 datapoints for each of the 40 unique samples for the *Partial Bandage* and the pulling EA. We split the 40 samples into a training (80%) and test samples (20%).

VI. EXPERIMENTS

In this section we evaluate the performance of EDO-Net, regarding its adaptation module f_ϕ , forward module g_θ and its generalisation capabilities. To this aim, we design the following experiments:

- 1) We examine how accurately we can decode physical properties from the latent representation z_i by learning to predict ground-truth parameters from z_i in simulation;
- 2) We quantitatively evaluate whether the latent representation z_i transfers between environments (from *Partial Bandage* to *Lifting*) or to different downstream tasks, such as learning an inverse model to predict the control action between two states in simulation;
- 3) We analyse the generalization capabilities of *EDO-Net* both in simulation and real-world environments, testing the model over a set of deformable objects with *unseen* elastic physical properties $\mathcal{T}_i \sim \mathcal{T}$.

We compare EDO-Net with a *Non-Conditioned* (NC) baseline model, which trains the forward model g_θ without conditioning on z_i . We also consider an ablation of EDO-Net trained on a single exploratory observation, rather than a sequence of interactions, which we denote by EDO1. Moreover, we additionally consider three oracle models in simulation to set an upper-bound performance for the tasks: two *Oracle* models conditioned on the ground-truth simulation parameters, respectively (OI) and (OF) for inverse and forward dynamics models, and an *Oracle Supervised* forward model (OS), trained with an additional supervised loss term over z_i , to directly predict the ground-truth simulation parameters during the training procedure.

A. Decoding Physical Properties

The aim of this section is two-fold: 1) to evaluate whether it is possible to decode from the latent representation z_i the ground truth physical properties \mathcal{T}_i of the deformable object, and 2) to analyse the influence of the length T of the sequence of exploratory observations used to extract z_i . In particular, we train an MLP with 3 hidden layers of size 64 and ReLU non-linearities which takes as input the learned representation z_i to predict the bending and elastic parameters of the simulator. We evaluate the predicted physical parameters in both the *Partial Bandage* and *Lifting* environments by evaluating the MSE between the ground truth normalized physical parameters and the model predictions. We distinguish between *seen* and *unseen* physical properties depending on whether $\mathcal{T}_i \sim \mathcal{T}$ was used to train the model or not. Fig. 6 shows the prediction results of the physical parameters from the learned z_i while varying the number T of exploratory observation O^i used to extract the representation. It can be noticed how increasing the number of observations improves the quality of the latent representation of the physical properties learned by f_ϕ , highlighting the relevance of using a sequence of dynamic interactions to encode physical properties. Moreover, the performance of EDO-Net is close to OS, suggesting that the self-supervised

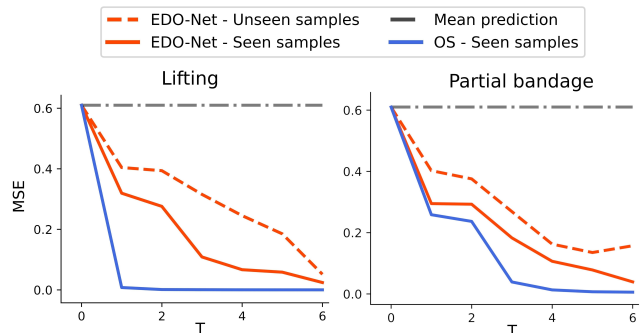


Fig. 6: MSE (in normalized units) for the prediction of the simulation parameters in the *Lifting* and *Partial bandage* environments, varying the length T of the sequence of exploratory observations.

loss implicitly trains the model to learn a latent representation of the physical properties without explicit supervision from the ground truth labels.

B. Evaluation of the Adaptation Module f_ϕ

In this section, we further evaluate z_i by answering the following questions: can we 1) transfer z_i to efficiently learn forward models of different environments, and 2) transfer z_i to efficiently learn new downstream tasks, such as inverse dynamics prediction? To address these questions we pretrain *EDO-Net* on the *Partial Bandage* environment and designed the following scenarios:

- 1) *Bandage2Lifting*: we fine-tune the forward dynamics model g'_θ on the *Lifting* environment, while keeping the weights of f_ϕ fixed;
- 2) *Inverse Dynamics*: we train an inverse dynamics model g''_θ conditioned on z_i in the *Partial Bandage* environment to predict the control action a_i^t between the initial state of the deformable object G_0^i and the next state G_t^i while keeping the weights of f_ϕ fixed.

In the *Bandage2Lifting* scenario, we evaluate the performance of the fine-tuned model by computing the MSE between the state-differences $\delta \hat{G}_i^{t+1}$ (in normalized units) and the ground-truth δG_i^{t+1} of the *Lifting* environment for deformable objects with physical properties $\mathcal{T}_i \sim \mathcal{T}$ unseen during training. For the *Inverse Dynamics* scenario, we implement g''_θ by initially encoding graph nodes and physical properties z_i with an MLP, subsequently projecting their concatenation to a latent space of the same dimensionality of the action. We finally aggregate and average the projections to obtain the predicted action. The performance of the inverse model is evaluated by computing the MSE between the normalized versions of the predicted action \hat{a}_i^t and the ground-truth action a_i^t . For both scenarios, we compare the model performance with the NC baseline, and EDO1. For the *Bandage2Lifting* scenario we set as reference performances EDO-Net model trained directly on the *Lifting* environment (EDO(L)-Net) and OF, while for the *Inverse Dynamics* scenario we set as reference performances OS and OI. The results are presented in Table I. We observe in the

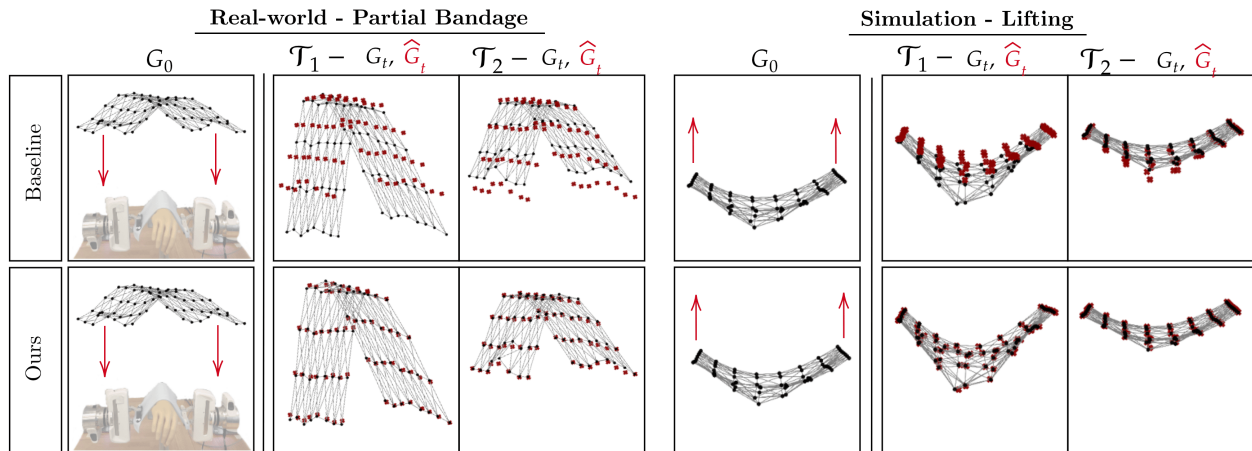


Fig. 7: Qualitative evaluation of the graph dynamics predictions \hat{G}_t obtained by EDO-Net and the NC baseline starting from the initial graph G_0 . For each environment we select two elastic samples with different physical properties $\mathcal{T}_1, \mathcal{T}_2$.

Bandage2Lifting scenario that all the evaluated models outperform the NC baseline, indicating that the representation z_i learned in the *Partial Bandage* environment carries relevant information for the *Lifting* one. For the *Inverse Dynamics* scenario, instead, we observe that EDO-Net outperforms all the other baseline methods. These results suggest that our latent representation transfers to different environments and downstream tasks.

C. Generalization to Unseen Physical Properties

In this section, we evaluate the generalisation capabilities of EDO-Net. We consider both simulation and real-world environments, and we perform quantitative and qualitative tests of the model over a set of deformable objects with elastic physical properties $\mathcal{T}_i \sim \mathcal{T}$ unseen during training. We evaluated the model performance by computing the MSE of the model’s predictions with respect to the ground truth for each testing sample. We compare the performance of our model with respect to the NC and the EDO1 baselines. In simulation we also compare to OS and OF. In Table II we report the mean and standard deviation of the MSEs evaluated across all the testing samples with physical properties $\mathcal{T}_i \sim \mathcal{T}$. In all scenarios, *EDO-Net* outperforms the baseline models both in terms of the average error and the standard deviation across samples with different elastic properties. The high standard deviation of the NC model is due to the large difference between the average elastic behavior and the extreme (rigid/elastic) ones. Moreover, *EDO-Net* achieves comparable performances with respect to OF. Qualitative

TABLE I: Results of *Bandage2Lifting* and *Inverse Dynamics* scenarios (in normalized units), with $T=5$. Lower is better.

(a) <i>Bandage2Lifting</i>		(b) <i>Inverse Dynamics</i>	
Model	MSE ($\times 10^{-3}$)	Model	MSE
NC	6.668 \pm 13.02	NC	9.705 \pm 11.11
EDO1	0.233 \pm 0.313	EDO1	0.212 \pm 0.331
EDO-Net	0.270 \pm 0.491	EDO-Net	0.058 \pm 0.096
EDO(L)-Net	0.102 \pm 0.068	OS	0.051 \pm 0.041
OF	0.081 \pm 0.040	OI	0.035 \pm 0.057

visualizations of the relevance of our proposed method for both simulation and real-world environment are shown in Fig. 7. We can observe how the NC baseline does not distinguish among samples with different physical properties (\mathcal{T}_1 and \mathcal{T}_2), hindering its capability of predicting the outcome of the robot control actions. On the other hand, *EDO-Net* successfully leverages the latent representations (z_1 and z_2) provided by the adaptation module f_ϕ .

TABLE II: Generalisation results of EDO-Net and the baselines in the simulated and real-world environments (in normalized units), with $T=5$. Lower is better.

Model	MSE ($\times 10^{-3}$) <i>Partial Bandage</i> simulation	MSE ($\times 10^{-3}$) <i>Lifting</i> simulation	MSE ($\times 10^{-3}$) <i>Partial Bandage</i> real world
NC	29.60 \pm 65.29	6.585 \pm 12.79	59.37 \pm 57.50
EDO1	0.260 \pm 0.197	0.171 \pm 0.106	3.046 \pm 1.603
EDO-Net	0.151 \pm 0.125	0.102 \pm 0.068	1.481 \pm 0.500
OS	0.992 \pm 1.480	0.321 \pm 0.699	–
OF	0.122 \pm 0.194	0.081 \pm 0.040	–

VII. CONCLUSIONS

We presented EDO-Net, a data-driven model to jointly learn a latent representation of physical properties of cloth-like deformable objects which is capable to generalize to unseen physical properties. We assessed in simulation that it is possible to decode ground truth parameters from the learned representation, as well as transfer it to different environments. Furthermore, we assessed both in simulation and real world how conditioning to the latent representation z_i helps the forward dynamics model in generalizing over unseen physical properties. The latent representation learned from EDO-Net is relevant for robotics tasks to generalize manipulation skills to a wide variety of cloth-like objects. Moreover, extending the framework to multiple exploration actions could enable learning physical properties beyond elasticity.

REFERENCES

- [1] S. Miller, J. Van Den Berg, M. Fritz, T. Darrell, K. Goldberg, and P. Abbeel, “A geometric approach to robotic laundry folding,” *The*

- International Journal of Robotics Research*, vol. 31, no. 2, pp. 249–267, 2012.
- [2] Z. Erickson, H. M. Clever, G. Turk, C. K. Liu, and C. C. Kemp, “Deep haptic model predictive control for robot-assisted dressing,” in *2018 IEEE international conference on robotics and automation (ICRA)*. IEEE, 2018, pp. 4437–4444.
 - [3] G. Canal, G. Alenyà, and C. Torras, “Adapting robot task planning to user preferences: an assistive shoe dressing example,” *Autonomous Robots*, vol. 43, no. 6, pp. 1343–1356, 2019.
 - [4] D. Seita, P. Florence, J. Tompson, E. Coumans, V. Sindhvani, K. Goldberg, and A. Zeng, “Learning to rearrange deformable cables, fabrics, and bags with goal-conditioned transporter networks,” in *2021 IEEE International Conference on Robotics and Automation (ICRA)*. IEEE, 2021, pp. 4568–4575.
 - [5] Z. Xu, J. Wu, A. Zeng, J. B. Tenenbaum, and S. Song, “Densephysnet: Learning dense physical object representations via multi-step dynamic interactions,” *arXiv preprint arXiv:1906.03853*, 2019.
 - [6] C. Wang, S. Wang, B. Romero, F. Veiga, and E. Adelson, “Swingbot: Learning physical features from in-hand tactile exploration for dynamic swing-up manipulation,” in *2020 IEEE/RSJ International Conference on Intelligent Robots and Systems (IROS)*. IEEE, 2020, pp. 5633–5640.
 - [7] J. Zhu, A. Cherubini, C. Dune, D. Navarro-Alarcon, F. Alambeigi, D. Berenson, F. Ficuciello, K. Harada, X. Li, J. Pan, *et al.*, “Challenges and outlook in robotic manipulation of deformable objects,” *arXiv preprint arXiv:2105.01767*, 2021.
 - [8] C. Chi, B. Burchfiel, E. Cousineau, S. Feng, and S. Song, “Iterative residual policy: for goal-conditioned dynamic manipulation of deformable objects,” *arXiv preprint arXiv:2203.00663*, 2022.
 - [9] Z. Weng, F. Paus, A. Varava, H. Yin, T. Asfour, and D. Kragic, “Graph-based task-specific prediction models for interactions between deformable and rigid objects,” in *2021 IEEE/RSJ International Conference on Intelligent Robots and Systems (IROS)*. IEEE, 2021, pp. 5741–5748.
 - [10] X. Lin, Y. Wang, Z. Huang, and D. Held, “Learning visible connectivity dynamics for cloth smoothing,” in *Conference on Robot Learning*. PMLR, 2022, pp. 256–266.
 - [11] X. Ma, D. Hsu, and W. S. Lee, “Learning latent graph dynamics for deformable object manipulation,” *arXiv preprint arXiv:2104.12149*, 2021.
 - [12] A. Sanchez-Gonzalez, J. Godwin, T. Pfaff, R. Ying, J. Leskovec, and P. Battaglia, “Learning to simulate complex physics with graph networks,” in *International Conference on Machine Learning*. PMLR, 2020, pp. 8459–8468.
 - [13] T. Pfaff, M. Fortunato, A. Sanchez-Gonzalez, and P. W. Battaglia, “Learning mesh-based simulation with graph networks,” *arXiv preprint arXiv:2010.03409*, 2020.
 - [14] A. Sanchez-Gonzalez, N. Heess, J. T. Springenberg, J. Merel, M. Riedmiller, R. Hadsell, and P. Battaglia, “Graph networks as learnable physics engines for inference and control,” in *International Conference on Machine Learning*. PMLR, 2018, pp. 4470–4479.
 - [15] M. McCloskey, “Intuitive physics,” *Scientific american*, vol. 248, no. 4, pp. 122–131, 1983.
 - [16] J. Wu, I. Yildirim, J. J. Lim, B. Freeman, and J. Tenenbaum, “Galileo: Perceiving physical object properties by integrating a physics engine with deep learning,” *Advances in neural information processing systems*, vol. 28, 2015.
 - [17] A. Longhini, M. C. Welle, I. Mitsioni, and D. Kragic, “Textile taxonomy and classification using pulling and twisting,” in *2021 IEEE/RSJ International Conference on Intelligent Robots and Systems (IROS)*. IEEE, 2021, pp. 7564–7571.
 - [18] P. Agrawal, A. V. Nair, P. Abbeel, J. Malik, and S. Levine, “Learning to poke by poking: Experiential learning of intuitive physics,” *Advances in neural information processing systems*, vol. 29, 2016.
 - [19] J. K. Li, W. S. Lee, and D. Hsu, “Push-net: Deep planar pushing for objects with unknown physical properties,” in *Robotics: Science and Systems*, vol. 14, 2018, pp. 1–9.
 - [20] P. Sundaresan, R. Antonova, and J. Bohg, “Diffcloud: Real-to-sim from point clouds with differentiable simulation and rendering of deformable objects,” *arXiv preprint arXiv:2204.03139*, 2022.
 - [21] W. Yan, A. Vangipuram, P. Abbeel, and L. Pinto, “Learning predictive representations for deformable objects using contrastive estimation,” *arXiv preprint arXiv:2003.05436*, 2020.
 - [22] M. Lippi, P. Poklukar, M. C. Welle, A. Varava, H. Yin, A. Marino, and D. Kragic, “Latent space roadmap for visual action planning of deformable and rigid object manipulation,” in *2020 IEEE/RSJ International Conference on Intelligent Robots and Systems (IROS)*. IEEE, 2020, pp. 5619–5626.
 - [23] —, “Enabling visual action planning for object manipulation through latent space roadmap,” *IEEE Transactions on Robotics*, 2022.
 - [24] S. Chen, Y. Liu, S. W. Yao, J. Li, T. Fan, and J. Pan, “Diffsr: Learning dynamical state representation for deformable object manipulation with differentiable simulation,” *IEEE Robotics and Automation Letters*, vol. 7, no. 4, pp. 9533–9540, 2022.
 - [25] A. Vaswani, N. Shazeer, N. Parmar, J. Uszkoreit, L. Jones, A. N. Gomez, Ł. Kaiser, and I. Polosukhin, “Attention is all you need,” *Advances in neural information processing systems*, vol. 30, 2017.
 - [26] P. Veličković, G. Cucurull, A. Casanova, A. Romero, P. Lio, and Y. Bengio, “Graph attention networks,” *arXiv preprint arXiv:1710.10903*, 2017.
 - [27] Y. Li, J. Wu, J.-Y. Zhu, J. B. Tenenbaum, A. Torralba, and R. Tedrake, “Propagation networks for model-based control under partial observation,” in *2019 International Conference on Robotics and Automation (ICRA)*. IEEE, 2019, pp. 1205–1211.
 - [28] S. Abu-El-Haija, B. Perozzi, A. Kapoor, N. Alipourfard, K. Lerman, H. Harutyunyan, G. Ver Steeg, and A. Galstyan, “Mixhop: Higher-order graph convolutional architectures via sparsified neighborhood mixing,” in *international conference on machine learning*. PMLR, 2019, pp. 21–29.
 - [29] E. Coumans and Y. Bai, “Pybullet, a python module for physics simulation for games, robotics and machine learning,” <http://pybullet.org>, 2016–2021.
 - [30] Z. Erickson, V. Gangaram, A. Kapusta, C. K. Liu, and C. C. Kemp, “Assistive gym: A physics simulation framework for assistive robotics,” in *2020 IEEE International Conference on Robotics and Automation (ICRA)*. IEEE, 2020, pp. 10 169–10 176.
 - [31] A. Savitzky and M. J. Golay, “Smoothing and differentiation of data by simplified least squares procedures,” *Analytical chemistry*, vol. 36, no. 8, pp. 1627–1639, 1964.
 - [32] A. Longhini, M. Moletta, A. Reichlin, M. C. Welle, A. Kravberg, Y. Wang, D. Held, Z. Erickson, and D. Kragic, “Elastic context: Encoding elasticity for data-driven models of textiles,” 2022. [Online]. Available: <https://arxiv.org/abs/2209.05428>
 - [33] D. E. Rumelhart, G. E. Hinton, and R. J. Williams, “Learning representations by back-propagating errors,” *nature*, vol. 323, no. 6088, pp. 533–536, 1986.
 - [34] D. P. Kingma and J. Ba, “Adam: A method for stochastic optimization,” *arXiv preprint arXiv:1412.6980*, 2014.